ICC

Iranian Chemical Communication

Original Research Article

Payame Noor University *http://icc.journals.pnu.ac.ir*

Synthesis of nanostructured palladium, palladium oxide and palladium-palladium oxide nanocomposite by the gel combustion method and application as catalyst for hydrogen revolution

Hassan Karami[a,b,*], Mohammad Ali Karimi[b,c], Ehsan Atin[c]

[a]*Nano Research Laboratory (NRL), Payame Noor University (PNU), P.O. BOX 97, Abhar, Iran*

[b]*Department of Chemistry, Payame Noor University, 19395-4697, Tehran, Iran*

[c]*Nanoscience and Nanotechnology Research Laboratory (NNRL), Department of Chemistry, Payame Noor University (PNU), Sirjan, Iran*

Received: 19 September 2015, Accepted: 29 February 2016, Published: 29 February 2016

Abstract

This paper presents a new gel combustion method to synthesize palladium nanoparticles, palladium oxide (PdO) nanoparticles and palladium-palladium oxide nanocomposites. In the proposed method, there are some effective parameters including palladium chloride concentration, polyvinyl alcohol (PVA) concentration, acid concentration, solvent composition and combustion temperature that their values are investigated and optimized by the "one at a time" method. The experimental data shows that the combustion temperature is the main factor that controls the sample composition to obtain palladium, palladium oxide or palladium-palladium nanocomposites. Characterization of the synthesized samples is performed by SEM, TEM, XRD and BET specific surface area measurements. The optimized sample consisted of clusters; each cluster is composed of smaller nanoparticles with an average diameter of 25 mm and 10 $m^2 . g^{-1}$ specific surface areas. The optimized Pd-PdO nanocomposite is successfully used as nanocatalyst for the hydrogen revolution.

Keywords: Palladium nanoparticles; palladium oxide nanoparticles; palladium-palladium oxide nanocomposite; gel combustion; catalyst; hydrogen revolution.

---

*Corresponding author: Hassan Karami
Tel: +98 (912) 5419727, Fax: +98 (242) 5226932
E-mail: karami_h@yahoo.com

Introduction

Great interest has been focused on the noble metal nanoparticles due to their interesting size- and shape dependent physical and chemical properties. They are technologically important in many fields such as catalysis [1,2], optics [3] and surface enhanced Raman spectroscopy [4,5]. Among metals, palladium is widely studied because of its optical, spectroscopic, magnetic and catalytic properties. The development of the new methods for the preparation of uniform palladium nanoparticles becomes a very important issue in heterogeneous catalysis and hydrogen storage materials. Palladium has an important role in chemical synthesis [6] and in many industrial applications[7,8]. Major of Pd applications requires very small and fine Pd particles where both the size and shape are critical parameters that should be controlled in order to maximize their efficiencies. For example, the reactivity and selectivity of a nanocatalyst can be tailored by controlling the shape, as it will determine the crystallographic facets exposed on the surface of a nanocrystal and therefore the number of atoms located at the edges or corners [9].

As a gas-sensing agent, palladium (Pd) has an interesting characteristic of hydrogen molecules, including the large capacity of hydrogen occlusion and the catalytic effect of the reaction between hydrogen and oxygen at room temperature. The Pd characteristics are very attractive for the hydrogen sensor for which the sensitivities are enhanced by down-sizing into the nanometer range [10]. Therefore, preparation of nano-structured Pd is also an active research field [11-13].

Several synthetic approaches and different palladium precursors have been applied to generate palladium nanoparticles having different shapes and sizes such as chemical reduction of $PdCl_2$ by $NaBH_4$ [14], arc-discharge [15], reduction of $Pd(OAc)_2$ in supercritical carbon dioxide [16], thermally induced reduction of $Pd(Fod)_2$ [17] and sonochemical reduction of $PdCl_2$ [18]. The size and shape of palladium nanoparticles have been discussed as a function of metal precursor concentration and of the effect of the surfactant molecules. However, the aqueous-phase synthesis of uniform nanoparticles by an environmentally-friendly process is still challenging.

Palladium oxide is the most important catalyst that is used for various reactions in the laboratory and industry. It has been used for catalytic oxidation of benzyl alcohol [19], sensing of OH radicals [20], oxidation of hydrocarbons [21], photocatalytic degradation of bacterial indicators, etc. [22].

There are many reports about the synthesis of Palladium nanocomposites such as palladium-polyaniline nanocomposite [23, 24], palladium-polycarbonate [25], palladium-silica [26], palladium-polypyrole [27], palladium-carbon nanotube [28], palladium-hematite [29], palladium-alumina [30], etc. The large number of reports about palladium nanocomposites reveals their importance in catalysts and sensors.

In this work, we present a new controllable method to synthesize Pd nanoparticles, PdO nanoparticles and Pd-PdO nanocomposites.

Experimental

Materials and reagents

All reagents and compounds were in analytical grade and obtained from Merck, Fluka and Loba Chimie (India). Double-distilled water was used in all experiments.

Instrumentals

Morphologies of the samples were characterized by scanning electron microscopy (Model XL-30, Philips, Netherland). Transmission electron microscope (Zeiss EM900, 80Kev) was used for determining the exact size and shape of particles. The composition and particles sizes of the samples were determined by XRD (E- Pert- MPD, Phillips, Netherland). The effective surface areas were determined by Brunauer-Emmet-Teller (BET) specific surface area measurements based on N_2 adsorption/desorption (Temcem 902 A Z Picc, Germany).

Procedure

Appropriate weight percent of palladium chloride was dissolved in a mixed solvent ethanol: HCl (0.1 M) (60:40). Then 8 g polyvinyl alcohol (PVA) was added into the obtained solution. The mixture was stirred until a transparent and homogeneous solution was obtained which called "sol". During sol formation, solution temperature should be kept lower than 80 ºC. After sol formation, the mixture was slowly heated to form a homogeneous gel. The obtained gel was heated until the complete solvent evaporation and the formation of a dried gel. The dried gel was pyrrolized at 500 ºC for 5 h. At this stage, aluminum and zinc salts were decomposed and converted to metal oxides. Aluminum oxide and zinc oxide were connected to form a nanocomposite. The obtained nanocomposites were studied by scanning electron microscopy (SEM), transmission electron microscopy (TEM), EDAX analysis, XRD patterns and Brunauer-Emmet-Teller (BET) specific surface area measurements. SEM and TEM instruments were used to define the morphology of the samples. XRD, TEM, SEM and BET were used for determining particles sizes. The compositions of the samples were measured by XRD and EDX analyses.

Results and discussion

In the present method, there are some effective parameters which can control the morphology, the particle sizes and the composition of the synthesized samples. The parameters include gel-making value, mixed solvent composition, pH, palladium salt value, and combustion temperature. The effect of each parameter was investigated and optimized by the one factor at a time method. In the following sections, the optimization experimental set is presented.

Effect of gel making value

Polyvinyl alcohol (PVA), generally used as suspension stabilizer, exhibits the effect of reducing particle size of the sample by decreasing the surface tension and by improving the dispersion of the reactants during the polymerization reaction [31]. Polyvinyl alcohol (PVA) is a hydrophilic polymer contributing hydroxyl group on each of its repeating units, which permits the development of hydrogen bonds with the hydroxyl and carboxyl groups of reactants [32]. PVA prolongs sedimentation reaction, causing particles to trammel in gel pores while the solvent evaporates silently and thus, not impacting again. In the gel combustion method, the gel network rigidity controls the morphology and the particle sizes of the synthesized sample to make a uniform nanostructured [33, 34]. In the gel structure, palladium chloride molecules were homogeneously dispersed through the polymeric network. Because of gel network rigidity, the dispersed molecules in the gel network cannot alter their positions. Therefore, during the combustion of the gel's layers, the palladium chloride molecules of the burnt layers combine with each other to create $PdCl_2$ particles. The formed particles are calcined to yield Pd, PdO or Pd-PdO nanocomposites during the pyrrolysis process. In these experiments, all samples were paralyzed at a constant combustion temperature (500 °C). XRD patterns showed that the amount of gel- making agent (PVA) has not any effect on the sample composition. In this temperature, all samples were in Pd-PdO nanocomposite form, including 50 wt% Pd and 50 %wt PdO. The PVA amount affects on the morphology and particle sizes of the samples. Figure 1 shows the SEM images of the samples that were synthesized by different content of PVA.

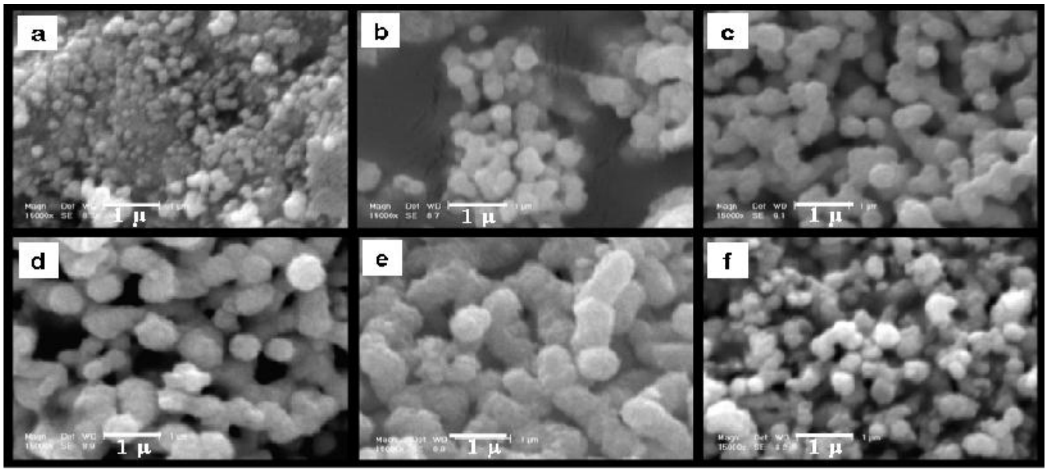

Figure 1. SEM images of Pd/PdO nanocomposites synthesized at different initial concentrations of PVA; 0 (a), 4 (b), 6 (c), 8 (d), 10 (e) and 12 %wt (f).

As it is visible in Figure 1, the PVA content changes considerably the morphology and particle sizes of the samples. The compact nanoparticles in the absence of PVA is converted to nanoporous rice shape clusters. The gel network is completed when the PVA content is increased from 0 to 10 %wt. At 10 %wt PVA, the gel network is complete and suitable to control the mechanism and kinetics of Pd-PdO nanocomposite particles. At lower PVA content, the gel network is not rigid enough. Because of the low solubility of PVA in ethanol-HCl solution, at higher content (12 %wt, Figure 1f); it is not obtained a uniform gel. Therefore, the sample doesn't have uniform morphology.

Effect of initial palladium salt content on the morphology and particle sizes

It is expected that the content of palladium chloride will have considerable effects on the morphology and particle sizes of Pd-PdO nanocomposites. For evaluation of this parameter, there was an attempt to synthesize some sample at different amounts of palladium chloride. Figure 2 shows the SEM images of the samples that were synthesized at 1, 2 and 3 %wt palladium chloride.

At the contents lower than 1 %wt, the amount of the final sample with respect to initial sol volume is very low so the sample weight is not enough for collecting and analysis. In addition, as Figure 2 shows, at low (1 %wt) and high (3 %wt) concentrations, the sample does not have uniform morphology. At high concentration (3 %wt), there are two reasons for decreasing of sample homogeneity.

Firstly, the ratio of salt to PVA is high, causing the gel network to be too weak to control the pyrrolysis and calcination processes. Secondly, the solubility of palladium chloride is low in ethanol-HCl mixed solution.

Solvent composition

Based on our previous experiences [33], ethanol-water is a suitable solvent to make PVA sol and PVA gel for synthesizing metal oxide nanoparticles. Initial experiments showed that palladium chloride does not have enough solubility in this solvent. According to chemistry facts, palladium chloride only has enough solubility in acidic media. Therefore, we used HCl solution mixed with ethanol as suitable solvent that both PVA and palladium chloride have enough solubility to make a uniform sol and consequently a uniform gel.

Figure 3 shows the effect of different concentrations of HCl on the morphology of the samples. At low concentration, palladium chloride does not have enough solubility. At 0.1 M HCl, the sample includes uniform nanoclusters made from uniform nanoseeds. At higher concentrations, the hydroxyl groups in PVA chains are protonated. The protonated PVA cannot make a polymeric gel to control the synthesis process.

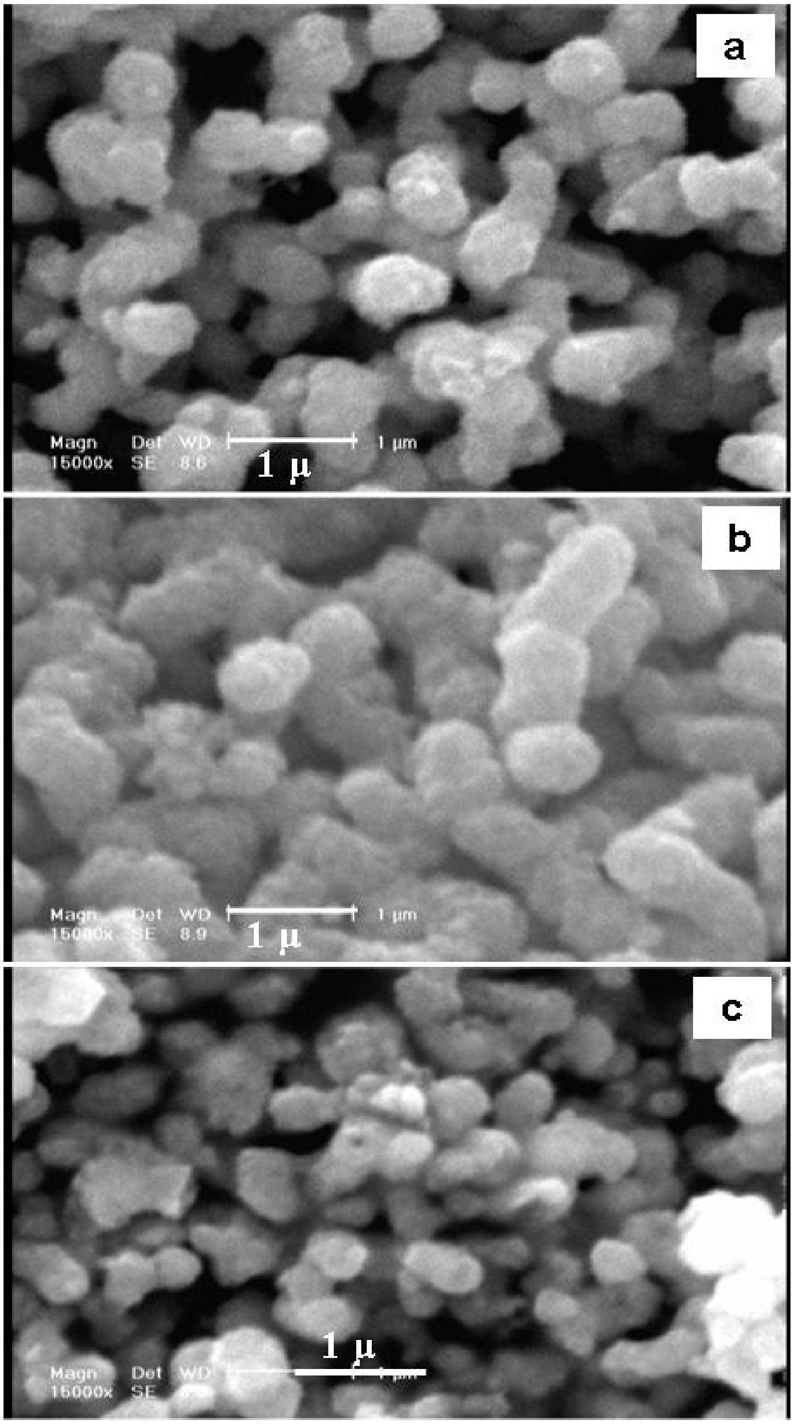

Figure 2. Effect of palladium chloride weight percentage (%wt) on the morphology and the particles sizes of the samples. The SEM images of samples with different palladium salt percentages of 1 %wt (a), 2 %wt (b) and 3 %wt (c).

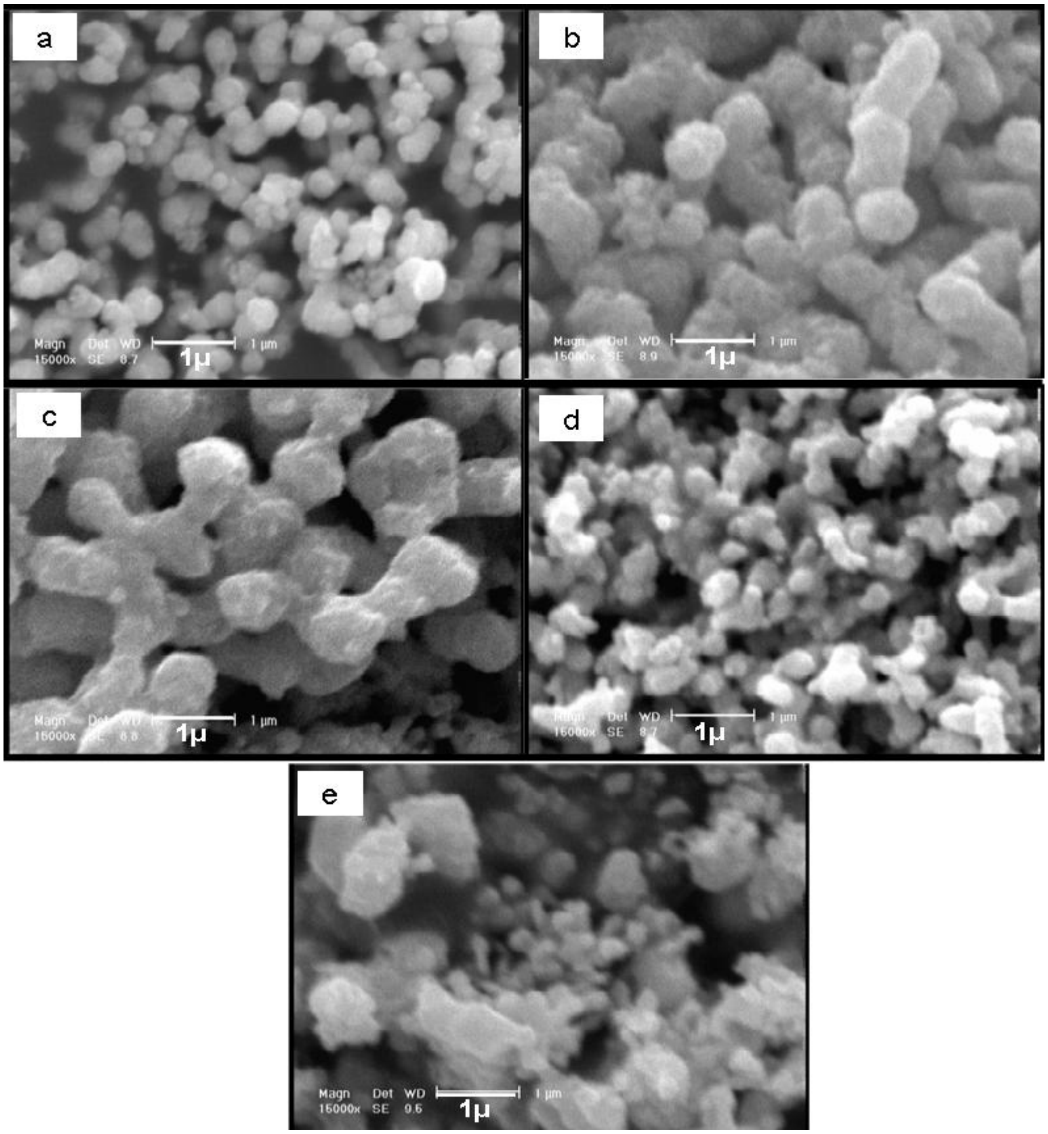

Figure 3. SEM images of different samples synthesized at different concentrations of hydrochloric acid; 0.05 M (a), 0.1 M (b), 0.5 M (c), 1 M (d) and 2 M (e). All SEM images are in same magnifications of 15000.

In the next step, the effect of ethanol/HCl solution ratio in a mixed solvent was investigated. Several samples were synthesized at different compositions of mixed solvents. The effect of solvent composition was shown in Figure 4 using SEM images.

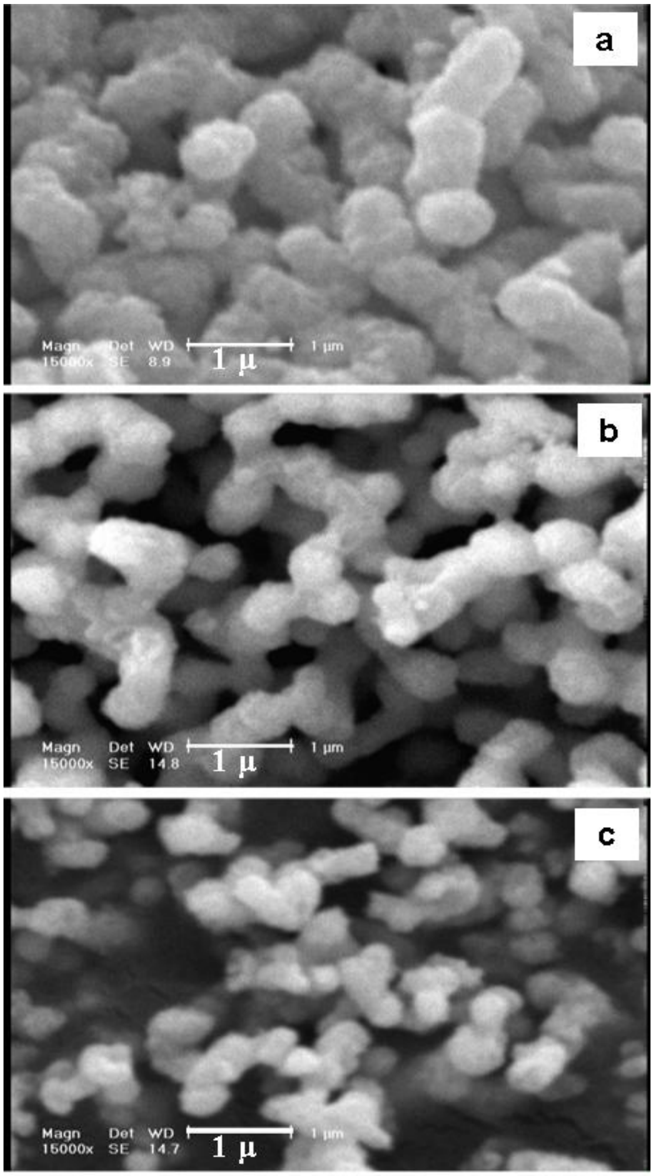

Figure 4. Effect of solvent composition on the SEM images of nanocomposite samples synthesized at 60:40 ethanol: HCl solution (a), 70:30 ethanol: HCl solution (b) and 80:20 ethanol: HCl solution (c) as solvent in the synthesis process.

The experimental results showed that in ethanol content lower than 60 %V/V, PVA has no solubility. At higher values, palladium chloride cannot completely dissolve. Based on the SEM images of Figure 4, the mixed solvent with 60 %V/V ethanol and 40 %V/V HCl solution is a suitable solvent to synthesize uniform nanoclusters.

Effect of pyrrolysis temperature

In the present method, during the pyrrolysis (combustion) process, organic gel network is burnt and the trapped palladium chloride molecules in holes in the polymeric network are calcinated and converted into palladium, palladium oxide or palladium-palladium oxide nanocomposites. The chemical reactions of the combustion step are as follows:

(eq. 1) $PdCl_2 \xrightarrow{Heat} Pd + Cl_2 \uparrow$

(eq. 2) $2\,PdCl_2 + O_2 \xrightarrow{Heat} 2PdO + 2Cl_2 \uparrow$

(eq. 3)

$$(m+n)PdCl_2 + \frac{1}{2}O_2 \xrightarrow{Heat} mPd.nPdO + 2Cl_2 \uparrow$$

The pyrrolysis temperature controls the share of each reaction (eqs. 1 to 3) in the final product. In equation 3, m and n can be varied as the synthesis temperature is changed.

First, the effect of pyrrolysis temperature was studied on the morphology of samples (Figure 5). As it can be seen in Figure 5, the morphology of the samples is changed considerably when the pyrrolysis temperature is increased from 400 to 600 °C. At lower temperatures (400 and 450 °C; Figures 5a and 5b), the clusters are compact and they don't have enough porosity. At these temperatures, calcination and particle growth rates are low because the combustion rate is low resulting in smaller particles of the samples. But, at lower temperature, the samples don’t have uniform nanoclusters.

At higher temperatures (550 and 600 °C; Figs. 5d and 5e), it can be seen that the samples consist large crystals. The presence of large crystals can be related to this fact that the combustion, calcination and particle growth rates are high. Therefore, the samples that are synthesized in these temperatures include agglomerated particles and large crystals. At 500 °C, combustion, calcination, nucleation and particle growth rates are suitable to form uniform nanoclusters (Figure 5c). Gel network is a control cage for palladium chloride molecules. When a gel is burned, burning rate is a limiting factor for the calcination rate of the salts and also a controller factor to reduce nucleation and particle growth [33].

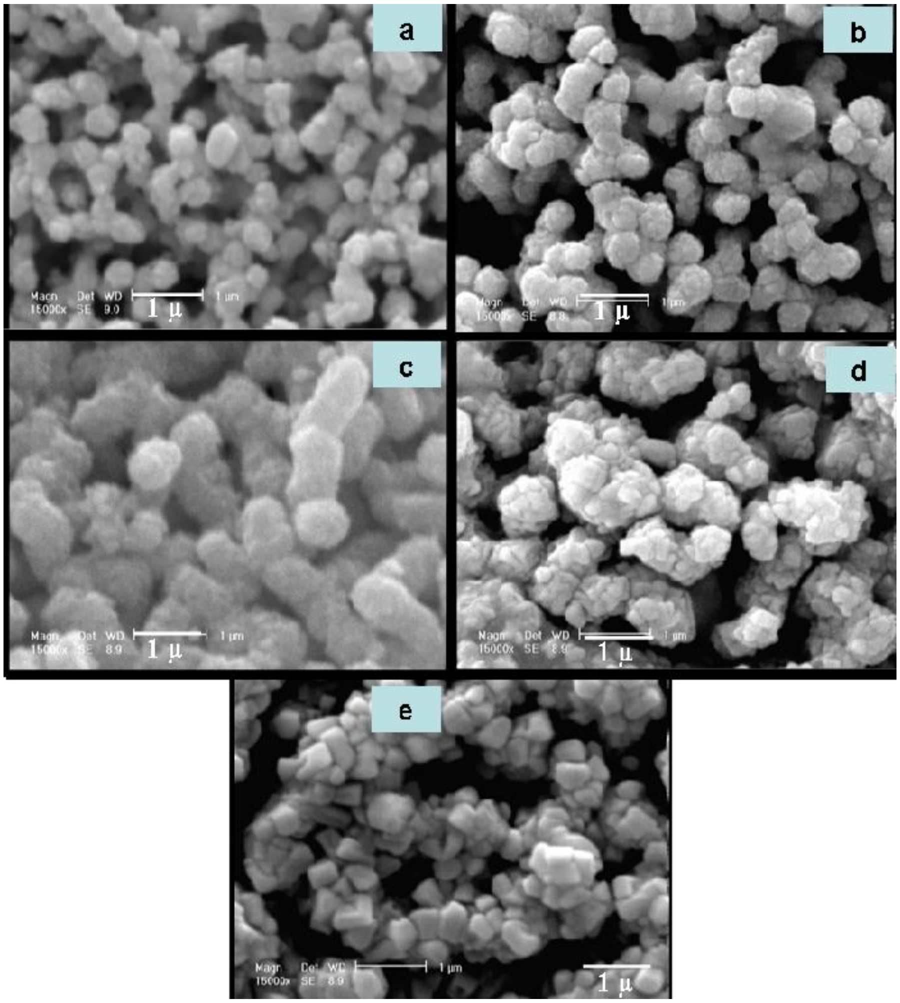

Figure 5. SEM images of the samples synthesized at different paralysis temperatures, including 400 °C (a), 450 °C (b), 500 °C (c), 550 °C (d) and 600 °C (e).

Figure 6 shows the TEM images of the sample synthesized at 500 °C. As it can be seen in Figure 6, the sample includes uniform and spherical nanoparticles with an average diameter of 25 nm.

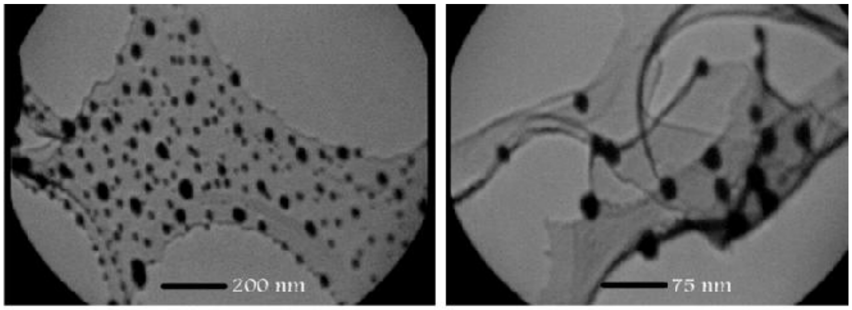

Figure 6. TEM images of Pd/PdO nanocomposite sample synthesized in the optimized conditions in two magnifications 20000 (left) and 70000 (right).

In the next step, the effect of pyrrolysis temperature was studied on the sample composition. Seven samples were synthesized at different temperatures under free atmosphere. The composition of the samples was characterized by XRD patterns. Figure 7 shows the XRD patterns of three samples (as some examples) that were synthesized at 400, 500 and 600 °C. As it can be seen in Figure 7, Pd content of the sample decreases when the pyrrolysis temperature is increased. The reason of this fact is clear. Under free atmosphere conditions, Pd reacts with oxygen to produce PdO. At lower temperatures, the oxidation reaction is negligible. On the other hand, PVA can act as a reducing agent to convert Pd^{2+} into Pd^0.

Figure 8 was drawn based on the XRD patterns of the samples synthesized at different temperatures. As Figure 8 shows, Pd content of the samples decreases when the pyrrolysis temperature is increased. At 350 °C, Pd content of the sample is more than 98 %wt and, at 700 °C, the Pd content is lower than 2 %wt. Based on the obtained results, the presented method is a powerful technique to synthesize Pd nanoparticles, PdO nanoparticles and Pd-PdO nanocomposites. By comparing the morphology, particles sizes and the composition of the samples that are synthesized at different pyrrolysis temperatures, it can be concluded that the introduced method is more suitable for preparation of Pd-PdO nanocomposites.

In the optimum conditions, the Pd/PdO nanocomposite sample includes uniform nanoclusters with uniform nanoseeds.

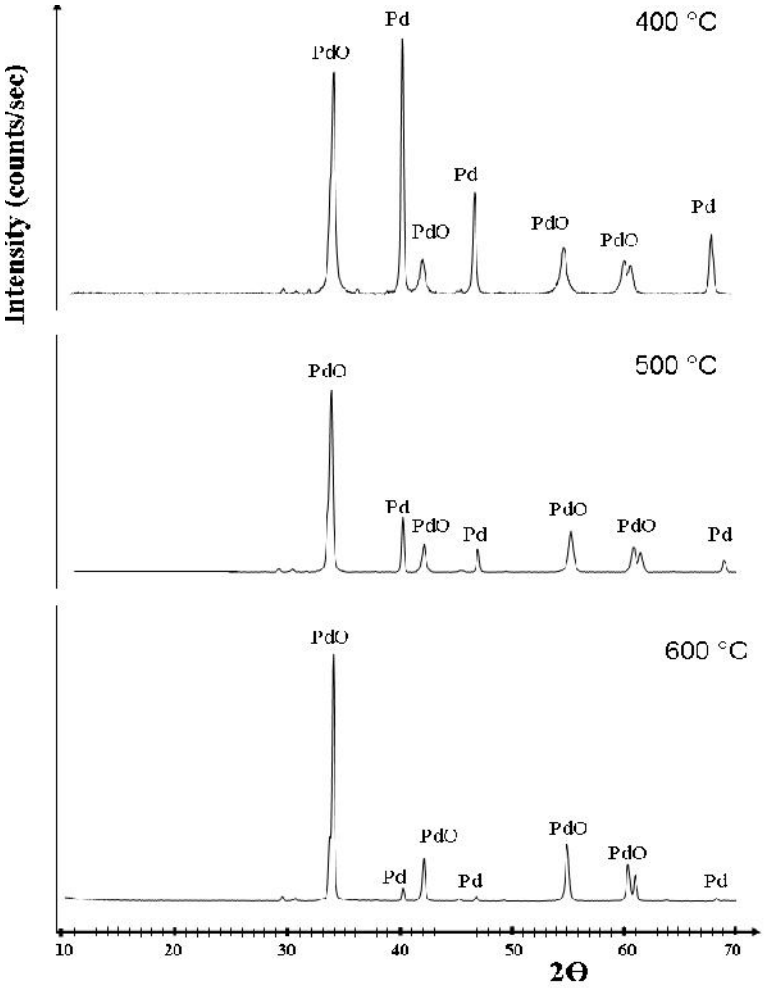

Figure 7. XRD patterns for the three Pd/PdO nanocomposite samples pyrrolized at different temperatures of 400, 500 and 600 ºC

Brunauer- Emmet- Teller (BET) specific surface area measurements were used for the determination of the pore volume, the specific surface area and the nanoparticles sizes. Based on the BET and BJH plots which were obtained based on N_2 gas adsorption/desorption isotherms, the sample has 10 $m^2.g^{-1}$ specific surface area and 19.5 nm average pore diameter.

Application as catalyst

The catalytic performance of the palladium-palladium oxide nanocomposite (50 %wt Pd and 50 %wt PdO) was studied by Cyclic Voltammetry for revolution of hydrogen in acidic solution. For this purpose, commercial palladium powder and the prepared palladium-palladium oxide nanocomposite were filled in the porosities of the graphite electrodes.

The obtained electrodes were used as working electrodes in cyclic Voltammetry experiments. The obtained cyclic voltammetric results for palladium-palladium oxide nanocomposite were compared with those of graphite and commercial palldium.

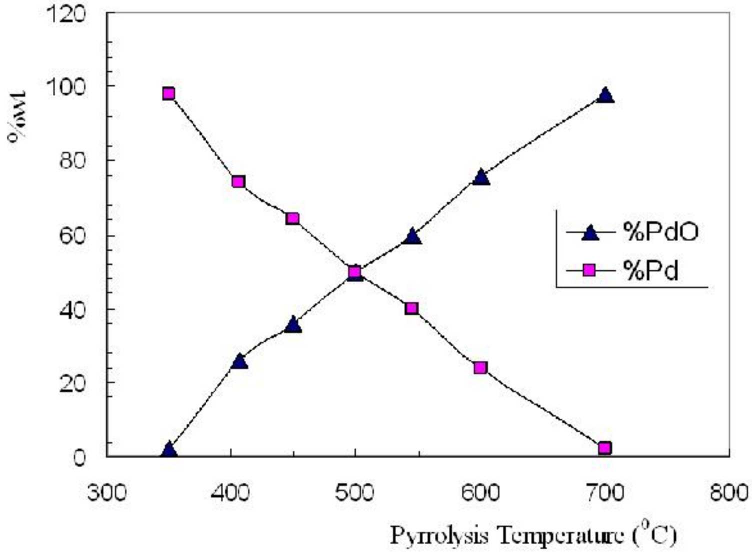

Figure 8. Effect of pyrrolysis temperature on the sample composition. Any of the samples does not have any impurity.

Figure 9 shows cyclic voltammograms of hydrogen reduction in sulfuric acid solution (1 M) on the different substrates (pure graphite, commercial palladium intercalated in graphite porosities and the synthesized palladium-palladium oxide nanocomposite intercalated in graphite porosities). As it can be seen in Figure 9, palladium-palladium oxide nanocomposite not only reduces reduction potential of hydrogen ions (positive shift), but also increases hydrogen revolution rate with respect to commercial palladium. Based on the obtained results for the catalytic performance of Pd/PdO nanocomposite, the prepared nanocomposite can be used as catalyst in fuel cells to facilitate and increase current densities of hydrogen reactions

An interesting phenomenon is considered on CV diagram taken by palladium-palladium oxide nanocomposite substrate; an oxidation peak was observed at 0.14 V versus Ag/AgCl reference electrode. Commercial palladium and also graphite substrates did not show this peak. The observed peak is related to oxidation of the adsorbed hydrogen gas. This peak reveals that palladium-palladium oxide nanocomposite has more capacity to adsorb hydrogen gas. Hydrogen ions are reduced during potential sweeping from 0.0 to -0.85 V. The realized hydrogen was strongly adsorbed by palladium-palladium oxide nanocomposite.

At oxidation sweep (from -0.3 to 0.3 V), the adsorbed hydrogen gas is oxidized to hydrogen ion. There is not any adsorption of realized hydrogen on the surface of graphite and commercial palladium or it is very weak. The strong adsorption of hydrogen gas on the surface of the nanocomposite helps to improve its catalytic performance.

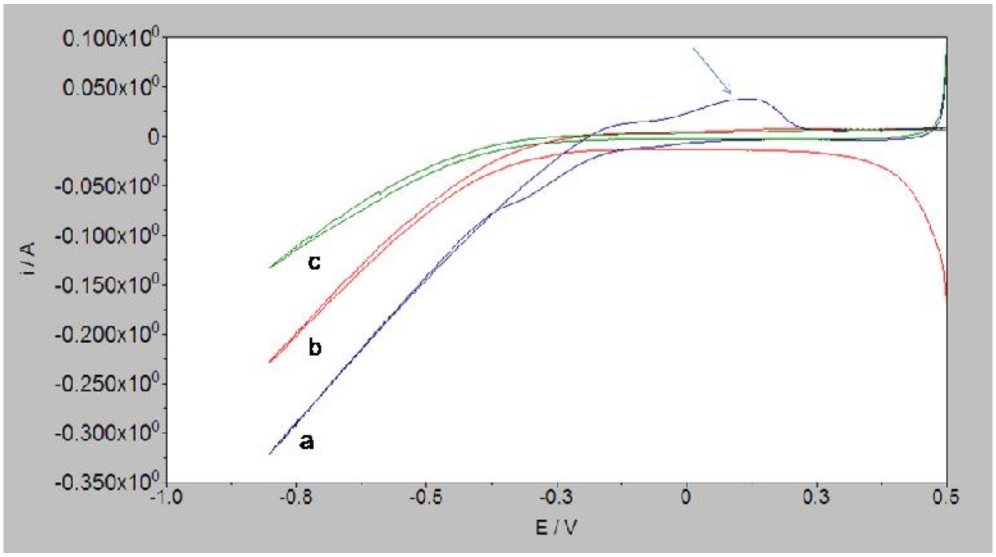

Figure 9. Cyclic voltammograms for hydrogen revolution in 1 M sulfuric acid on the surface of palladium-palladium nanocomposite (a), commercial palladium power and pure graphite (c). All potential were recorded versus Ag/AgCl reference electrode. Commercial palladium and palladium-palladium nanocomposite powders were intercalated (filled) on the graphite pores. The filled graphite electrodes were used as working electrodes.

Conclusion

A gel combustion method based on PVA as a gel-masking agent can be used as a powerful method to synthesize PdO, Pd and their nanocomposites. In this procedure, Pd, PdO and their nanocomposites were synthesized with the more specific surface area. They were expected to have some improved ability in gas sensing and photocatalytic applications. Palladium nanoparticles can be successfully used as nanocatalyst to catalyze hydrogen generation in acid media.

Acknowledgments

We gratefully acknowledge the support of this research by Payame Noor University Research Council.

References

[1] R.M. Rioux, H. Song, M. Grass, S. Habas, K. Niesz, J.D. Hoefelmeyer P. Yang, G.A. Somorjai, *Top. Catal.*, **2006**, *39*, 167-173.

[2] A.L. Stepanov, A.N. Golubev, S.I. Nikitin, Y.N. Osin, *Rev. Adv. Mater. Sci.*, **2014**, *38*, 160-175.

[3] Y. Seol, A.E. Carpenter, T.T. Perkins, *Opt. Lett.* **2006**, *31*, 2429-2431.

[4] Z.Q. Tian, B. Ren, D.Y. Wu, *J. Phys. Chem. B*, **2002**, *106*, 9463-9483.

[5] S.W. Han, K.Y. Lee, *Korean Chem. Soc.* **2005**, *26*, 1427-1430.

[6] B. Woodward, *Platinum Metals Rev.*, **2012**, *56*, 213-217.

Y. Nishihata, J. Mizuki, T. Akao, H. Tanaka, M. Uenishi, M. Kimura, T. Okamoto, N. Hamada, *Nature,* **2002**, *418*, 164-167.

[7] C.P.K. Rao, D.C. Trivedi, *Coordin. Chem. Rev.*, **2005**, *249*, 613-631.

[8] Y. Sun, Z. Tao, J. Chen, T. Herricks, Y. Xia, *J. Am. Chem. Soc.* **2004**, *126*, 5940-5941.

[9] A. Kolmakov, D.O. Klenov, Y. Lilach, S. Stemmer, M. Moskovits, *Nano Lett.* **2005**, *5*, 667-673.

[10] J. Chen, B. Wiley, J. McLellan, Y. Xiong, Z. Li, Y. Xia, *Nano Lett.* **2005**, *5*, 2058-2062.

[11] Y. Sekiguchi, Y. Hayashi, H. Takizawa, *Mater. T. JIM.*, **2011**, *52*, 1048-1052.

[12] J. Cookson, *Platinum metals Rev.*, **2012**, *56*, 83-98.

[13] T. Tsuji, K. Iryo, H. Ohta, Y. Nishimura, *Jpn. J. Appl. Phys.*, **2000**, *39*, 981-983.

[14] N.R. Jana, Z.L. Wang, T. Pal, *Langmuir*, **2000**, *16*, 2457-2463.

[15] D. Bera, S.C. Kuiry, M. McCutchen, A. Kruize, H. Heinrich, M. Meyyappan, S. Seal, *Chem. Phys. Lett.*, **2004**, *386*, 364-368.

[16] A. Kameo, T. Yoshimura, K. Esumi, *Colloid Surf. A*, **2003**, *215*, 181-189.

[17] P.F. Ho, K.M. Chi, *Nanotechnology*, **2004**, *15*, 1059-1064.

[18] K. Okitsu, H. Bandow, Y. Maeda, *Chem. Mater.*, **1996**, *8*, 315-317.

[19] K. Wada, K. Yano, T. Kondo, T.A. Mitsudo, *Catalysis Today*, **2006,** *117*, 242-247.

[20] J. Liu, G. Lagger, P. Tacchini, H. Girault, *J. Electroanal. Chem.*,

2008, *131*, 619-620.

[21] G. Postole, B. Bonnetot, A. Gervasini, C. Guimon, A. Auroux, N.I. Lonescu, M. Caldararu, *Appl. Catalysis A*, **2007**, *316*, 250-258.

[22] P. Wu, R. Xie, J.A. Imlay, J.K. Shang, *Appl. Catalyst B*, **2009**, *88*, 576-581.

[23] A.A. Athawalie, S.V. Bhaghwat, B.B. Katre, *Sens. Actuators B*, **2006**, *114*, 263-267.

[24] S. Ivanov, U. Lange, V. Tsakova, V.M. Virsky, *Sens. Actuators B*, **2010**, *150*, 271-278.

[25] O.P. Valmikanathan, O. Ostroverkhova, I.S. Mulla, K. Vijayamohanan, S.V. Atre, *Polymer*, **2008,** *49*, 3413-3418.

[26] Elvan Sari, Manhoe Kim, Steven O. Salley, K.Y. Simon Ng, *Appl. Catalysis A*, **2013**, *467*, 261-269.

[27] L. Hong, Y. Li, M. Yang, *Sens. Actuators B*, **2010**, *145*, 25-31.

[28] Z. Li, J. Li, X. Wu, S. Shuang, C. Dong, M.M. Choi, *Sens. Actuators B*, **2009**, *139*, 453-461.

[29] H. Liu, M. Liang, C. Xiao, N. Zheng, X. Feng, Y. Liu, J. Xie, Y. Wang, *J. Molec. Catalysis A*, **2009**, *308*, 79-86.

[30] A.L. Ahmed, N.N.N. Mustafa, *Int. J. Hydr. Ener.* **2007**, *32*, 2010-2021.

[31] J.S. Kim, C. Han, J.H. Wee, *Talanta*, **2006**, *68*, 963-968.

[32] P. Fatehi, H. Xiao, *Colloids Surf. A: Physicochem. Eng. Aspects*, **2008**, *327*, 127-133.

[33] H. Karami, A. Aminifar, H. Tavallali, Z. Namdar, *J. Clust. Sci.* **2010**, *21*, 1-9.

[34] H. Karami, *Int. J. Electrochem. Sci.* **2010**, *5*, 720-730.